Bio-evaluation and molecular modeling studies of ARG-TRP-ARG-based peptides as antimicrobial agents

[ID]Emmanuel T. Akintayo[1], [ID]Olaoye Stella[1], [ID]Sunday Adewale Akintelu[2], [ID]Abel Kolawole Oyebamiji[3,4*]
[1]Department of Chemistry, Ekiti State University. Ado-Ekiti, Nigeria; emmanuelakintayo@eksu.edu.ng (E.T.A.).
[2]School of Chemistry and Physics, University of KwaZulu-Natal, Durban, South Africa.
[3]Department of Industrial Chemistry, University of Ilesa, Ilesa, Osun State, Nigeria; abel_oyebamiji@unilesa.edu.ng (A.K.O.).
[4]Good Health and Wellbeing Research Clusters (SDG 03), University of Ilesa, Ilesa, Osun State, Nigeria.

Abstract: The battle against bacterial infections in both young and elderly populations continues to be a focus for researchers worldwide. This issue has led to the discovery of the most effective antibacterial ARG-TRP-ARG-based peptides through density functional theory and molecular modeling analysis. In this research, the inhibitory effectiveness of an ARG-TRP-ARG-based peptide was evaluated using in silico methods. The optimization was carried out with density functional theory, while molecular modeling studies were performed using induced-fit docking and molecular dynamics simulations. Compounds 3 and 4 showed promising responses regarding their HOMO energy, with compound 3 displaying a stronger propensity for favorable reactions in terms of energy gap. It was noted that compound 10, which possessed the lowest LUMO energy value, had the highest ability to accept electrons from nearby compounds. Additionally, when testing the compounds against thymidylate kinase from gram-positive bacteria (4HLC) and gyrase B from Thermus thermophilus (1KIJ), compounds 9 and 5 demonstrated the most significant inhibition of the targeted receptors. Molecular dynamics simulations confirmed the effectiveness of the lead compounds as predicted by the docking approach. Furthermore, the binding affinities were predicted from the calculated descriptors using Python (v3.11), and the results were presented accordingly.

Keywords: Affinity, Amino acids, Bacterial, Drugs, Insilico.

1. Introduction

The reports by various scientists have revealed peptides as effective disease-fighting agents with numerous biological roles. These agents are used as drugs to cure various conditions, such as hormonal issues, bacterial infections, tumors, and metabolic disorders. In 1920, reports showed that scientists discovered insulin as the first peptide-based drug [1, 2]. This class of drugs is viewed as fairly contemporary and comprehensive, featuring more than 60 approved healing agents globally, along with around 400 additional agents currently in clinical trials [1-3]. The attractiveness of peptides arises from their remarkable specificity and effectiveness, commonly ascribed to their capacity to target protein–protein interactions that small compounds are unable to handle. There are, however, several shortcomings associated with peptide-based medications, including their limited stability due to degradation by proteases, brief half-lives, low oral bioavailability, and inadequate cell permeability [4]. In tackling these challenges, novel drug designs such as terminal modifications and lipid attachments, along with drug delivery techniques combined with computational support approaches, have been suggested to improve stability, affinity, and specificity [5-7].

Bacteria are essential organisms for human existence. They contribute significantly to numerous aspects related to health, bioengineering, and the environment [8]. Also, they play a crucial role in

essential nutrient cycles; certain types of bacteria convert atmospheric nitrogen into forms that can be absorbed by plants, while decomposers effectively reprocess carbon, phosphorus, sulfur, and other elements. Moreover, this stabilization and recycling of nutrients are important for a stable ecosystem. According to Bonadonna et al. [9], many enzymes and drugs have been produced from bacterial modification, and this is considered advantageous due to the swift duplication rate of bacteria and the probability of designing nearly limitless bacterial genomes. Also, as reported by many scientists, there is a need for efficient drug-like compounds to curb bacterial resistance among humans [10-12]. This work is therefore aimed at investigating the biochemical mechanism and analysis of ARG-TRP-ARG-based peptides against Gram-positive thymidylate kinase (4hlc) [13] and Thermus thermophilus gyrase B (1kij) [14].

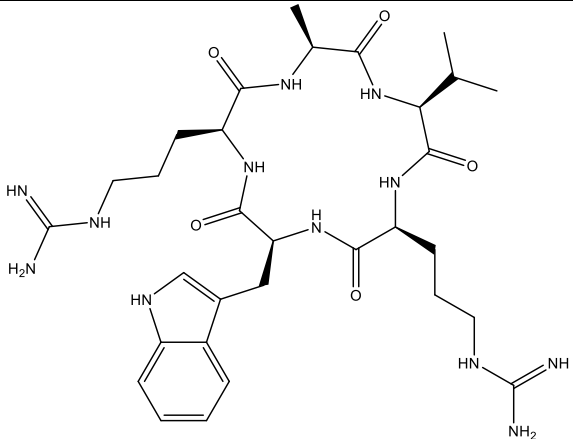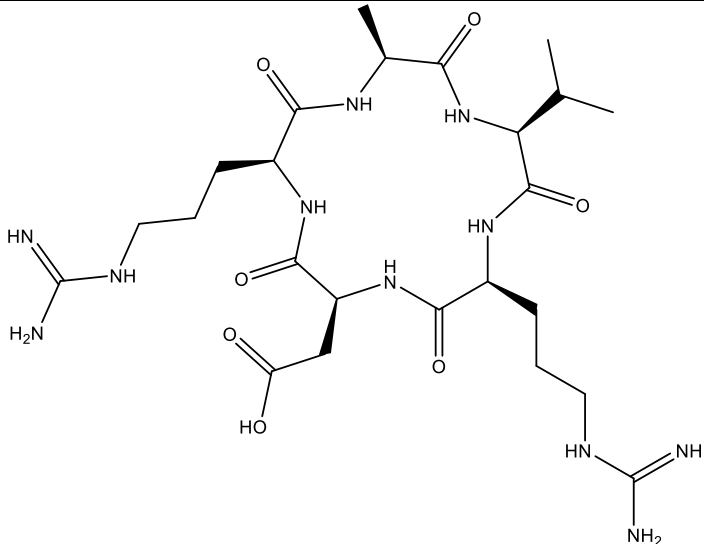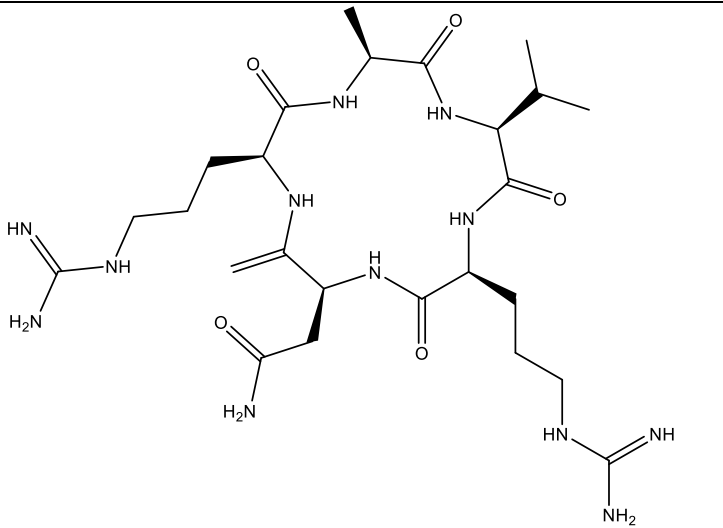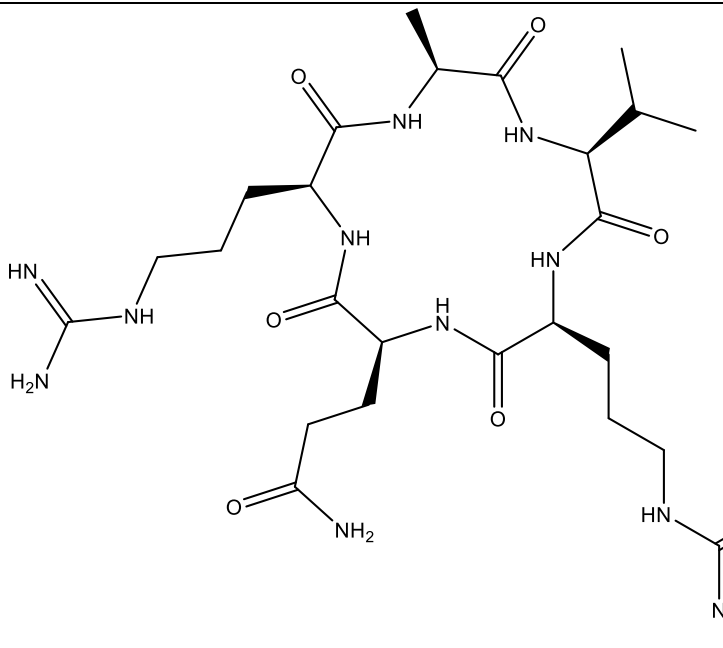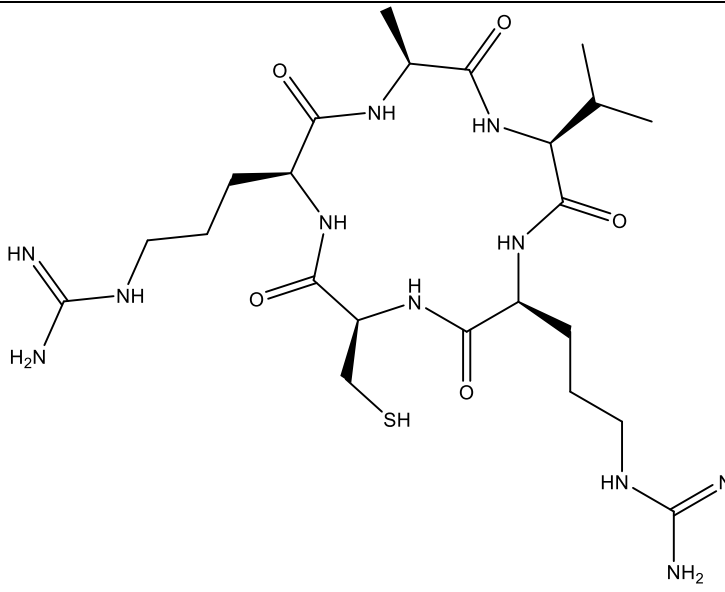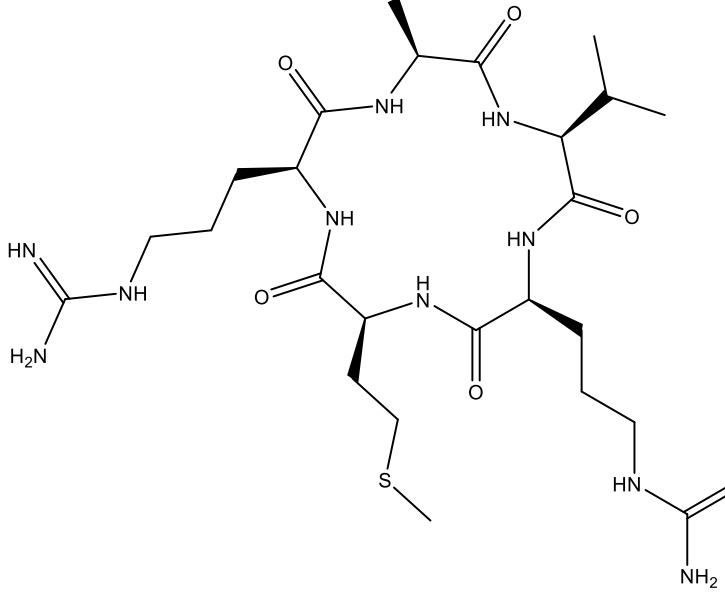## 2. Materials and Methods

2.1. Ligand Optimization

Two-dimensional structures of eleven compounds were modeled using ChemDraw 22.2.0 version, and they were further converted to three-dimensional structures for optimization and minimization processes using the density functional theory method via Spartan 14 software [15]. The compounds were assessed in vacuum, and energy and equilibrium geometry calculations at the ground state were performed from their current geometry, featuring a neutral charge with zero (0) unpaired electrons. The optimization completion of the analyzed ligands was found to depend on the number of atoms in the compounds. Therefore, several descriptors that explain the activities and reactivity of the studied compounds were presented and prepared for additional analysis.
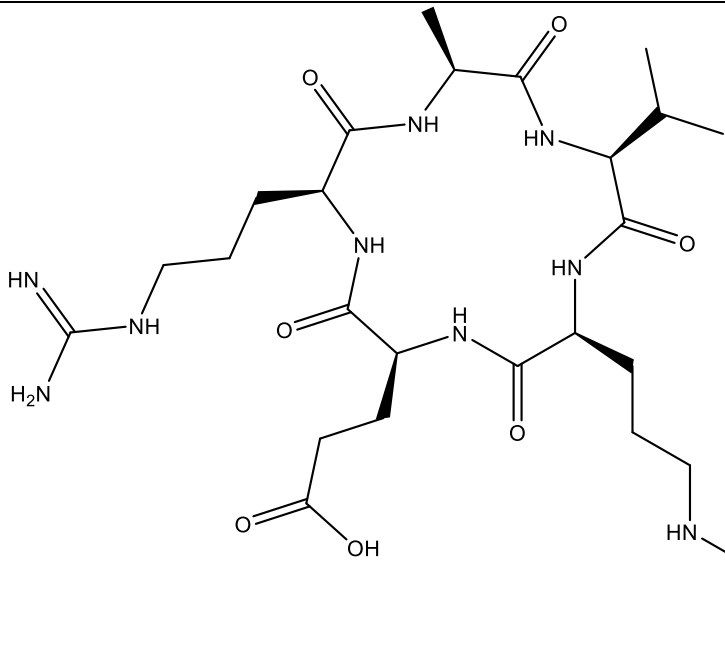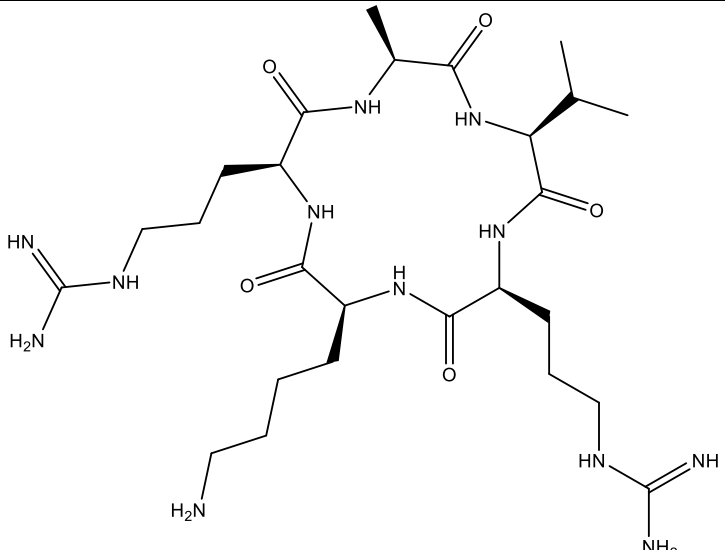
The IUPAC name of the studied compound and its 2-D structures are shown in Table 1.
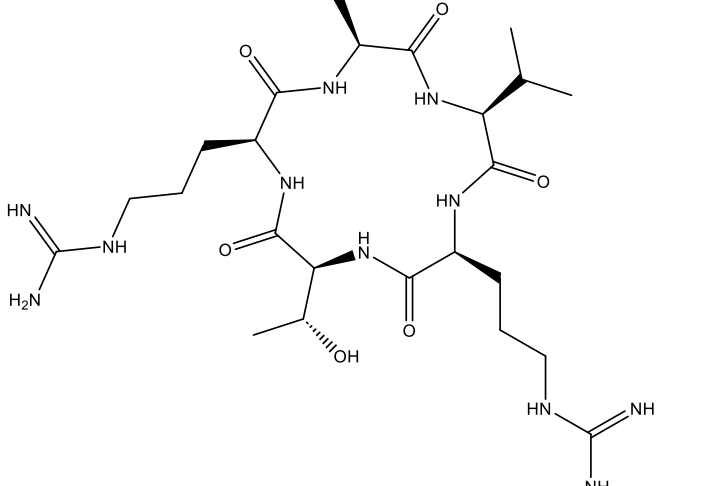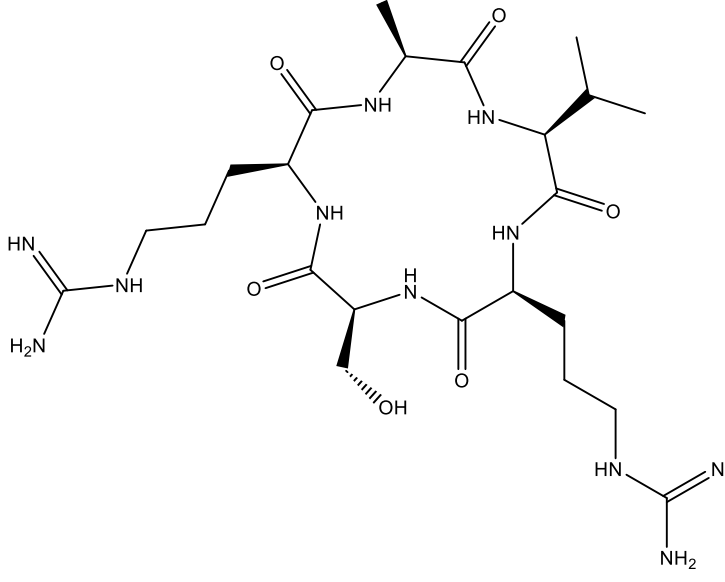
Table 1.
Two-dimensional structure of the studied compounds.
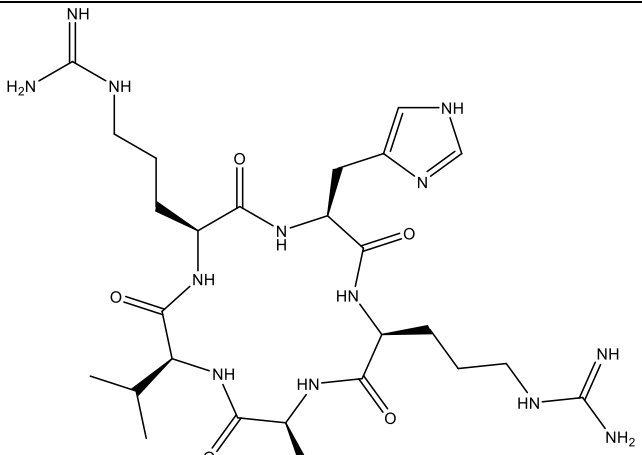
	2-Dimension	IUPAC Name
1		1,1'-(((2S,5S,8S,11S,14S)-5-((1H-indol-3-yl) methyl)-14-isopropyl-11-methyl-3,6,9,12,15-pentaoxo-1,4,7,10,13-pentaazacyclopentadecane-2,8-diyl) bis(propane-3,1-diyl)) diguanidine
2		2-((2S,5S,8S,11S,14S)-5,14-bis(3-guanidinopropyl)-11-isopropyl-8-methyl-3,6,9,12,15-pentaoxo-1,4,7,10,13-pentaazacyclopentadecan-2-yl) acetic acid

| 3 | | 2-((2S,5S,8S,11S,14S)-5,14-bis(3-guanidinopropyl)-11-isopropyl-8-methyl-3-methylene-6,9,12,15-tetraoxo-1,4,7,10,13-pentaazacyclopentadecan-2-yl)acetamide |
| 4 | | 3-((2S,5S,8S,11S,14S)-5,14-bis(3-guanidinopropyl)-11-isopropyl-8-methyl-3,6,9,12,15-pentaoxo-1,4,7,10,13-pentaazacyclopentadecan-2-yl)propanamide |

| 5 | | 1,1'-(((2S,5R,8S,11S,14S)-14-isopropyl-5-(mercaptomethyl)-11-methyl-3,6,9,12,15-pentaoxo-1,4,7,10,13-pentaazacyclopentadecane-2,8-diyl) bis(propane-3,1-diyl)) diguanidine |
| 6 | | 1,1'-(((2S,5S,8S,11S,14S)-14-isopropyl-11-methyl-5-(2-(methylthio) ethyl)-3,6,9,12,15-pentaoxo-1,4,7,10,13-pentaazacyclopentadecane-2,8-diyl) bis(propane-3,1-diyl)) diguanidine |

| 7 | | 3-((2S,5S,8S,11S,14S)-5,14-bis(3-guanidinopropyl)-11-isopropyl-8-methyl-3,6,9,12,15-pentaoxo-1,4,7,10,13-pentaazacyclopentadecan-2-yl) propanoic acid |
| 8 | | 1,1'-(((2S,5S,8S,11S,14S)-5-(4-aminobutyl)-14-isopropyl-11-methyl-3,6,9,12,15-pentaoxo-1,4,7,10,13-pentaazacyclopentadecane-2,8-diyl) bis(propane-3,1-diyl)) diguanidine |

| 9 | | 1,1'-(((2S,5S,8S,11S,14S)-5-((R)-1-hydroxyethyl)-14-isopropyl-11-methyl-3,6,9,12,15-pentaoxo-1,4,7,10,13-pentaazacyclopentadecane-2,8-diyl) bis (propane-3,1-diyl)) diguanidine |
| 10 | | 1,1'-(((2S,5S,8S,11S,14S)-5-(hydroxymethyl)-14-isopropyl-11-methyl-3,6,9,12,15-pentaoxo-1,4,7,10,13-pentaazacyclopentadecane-2,8-diyl) bis(propane-3,1-diyl)) diguanidine |

| 11 |
 | 1,1'-(((2S,5S,8S,11S,14S)-5-((1H-imidazol-4-yl) methyl)-14-isopropyl-11-methyl-3,6,9,12,15-pentaoxo-1,4,7,10,13-pentaazacyclopentadecane-2,8-diyl) bis(propane-3,1-diyl)) diguanidine |

2.2. Induced-Fit Docking Examination

In this study, eleven peptide-based compounds were optimized and further refined using the Quikprep tool within molecular operating environments (MOE), and the results were saved in .moe format for subsequent docking analysis. Additionally, thymidylate kinase from gram-positive bacteria (4HLC) and gyrase B from Thermus thermophilus (1KIJ) were retrieved from the Protein Data Bank and processed with the sequence editor to eliminate water molecules and any small molecules that accompanied the receptors. The cleaned receptors were then repaired using the QuickPrep tool before determining the binding site location. The potential binding sites for the two receptors were identified based on factors such as ligand binding propensity (PLB), dimensions, hydrophobic areas, surface features, and relevant amino acid residues, utilizing the SiteFinder tool. The processed and prepared protein structures were saved in .moe format in preparation for docking calculations using the induced fit approach. The results obtained from the docked complexes were reported in kcal/mol, and the types of interactions present in the docked complexes were documented and presented.

2.3. Binding Affinity Prediction

In this work, the binding affinity of the studied compounds was predicted using HOMO, LUMO, and energy gap (descriptors generated from optimized studied structures). The connection between the three features linked to the predicted binding affinity obtained from the docking of the studied compounds against Gram-positive thymidylate kinase (4HLC) and Gram-negative gyrase B (1KIJ) was investigated using a decision tree regressor [16].

2.4. Model Training and Optimization

The potential non-linear connection between the calculated descriptors and the predicted binding affinity was analyzed using a Decision Tree Regressor (Scikit-learn v1.4.2). Hyperparameter optimization of the model was performed using Grid Search combined with Leave-One-Out Cross-Validation (LOOCV). The reliability of the developed model was assessed through LOOCV MAE, the Coefficient of Determination (R^2), and comparison against a baseline predictor (mean binding affinity). Finally, the implementation of the workflow in Python (v3.11) was achieved using these methods: Pandas, Scikit-learn and Matplotlib [17].

3. Results and Discussion

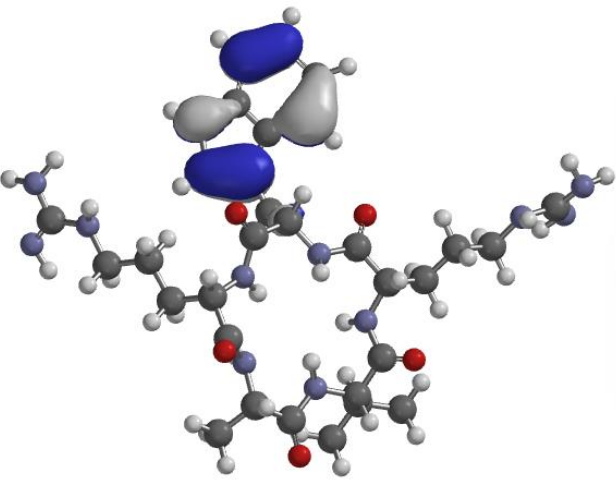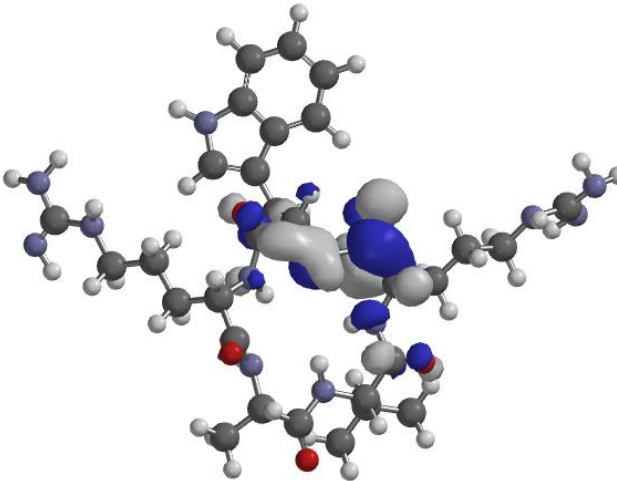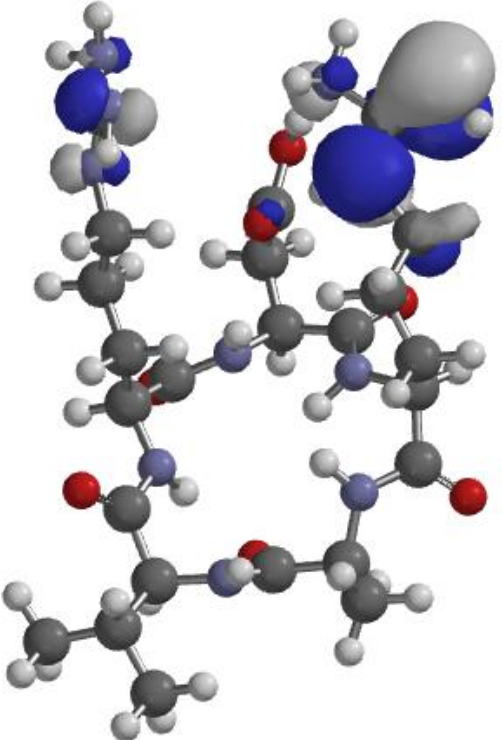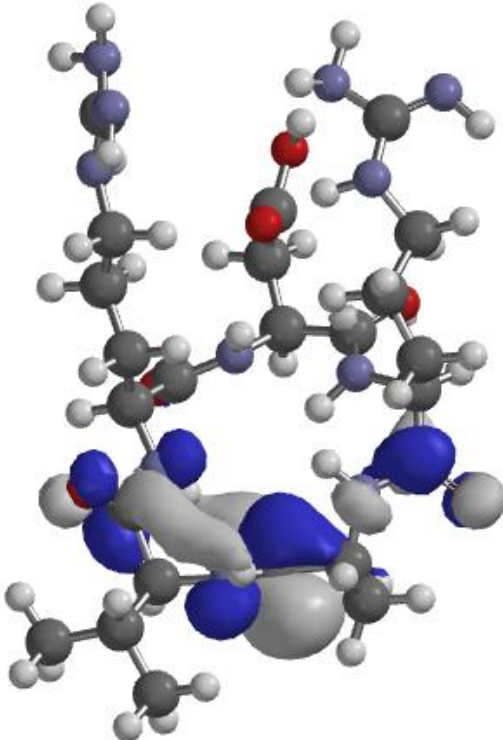### 3.1. Calculated Features of the Studied Compounds

The examined compounds in this work generated various descriptors that predict their potential reactivity. Table 2 presents the highest occupied molecular orbital energy (HOMO energy), the lowest unoccupied molecular orbital energy (LUMO energy), and the energy gap. The HOMO energy indicates the ability of a reacting compound to donate electrons to nearby molecules; that is, the higher the HOMO energy value, the greater the compound's capacity to donate electrons. Accordingly, 2-((2S,5S,8S,11S,14S)-5,14-bis(3-guanidinopropyl)-11-isopropyl-8-methyl-3-methylene-6,9,12,15-tetraoxo-1,4,7,10,13-pentaazacyclopentadecan-2-yl)acetamide (Compound **3**) and 3-((2S,5S,8S,11S,14S)-5,14-bis(3-guanidinopropyl)-11-isopropyl-8-methyl-3,6,9,12,15-pentaoxo-1,4,7,10,13-pentaazacyclopentadecan-2-yl)propanamide (Compound **4**) were observed to have the potential to react effectively according to their HOMO energies. This reactivity, as indicated by HOMO energy, can be attributed to the presence of amide groups in compounds 3 and 4. As stated by various researchers [15, 18], the presence of electron-withdrawing carbonyl groups and electron-donating nitrogen in a compound facilitates the stabilization of charge during the transfer of electrons between compounds. Consequently, the combination of these two influences in compounds **3** and **4** permitted the adjustment of electron density in adjacent π-systems, which thereby refined their redox potential. Furthermore, the ability of any compound to receive electrons from any nearby compound also plays a crucial role in the reactivity of any compound; therefore, as shown in Table 2, it was observed that compound 10 (1,1'-(((2S,5S,8S,11S,14S)-5-(hydroxymethyl)-14-isopropyl-11-methyl-3,6,9,12,15-pentaoxo-1,4,7,10,13-pentaazacyclopentadecane-2,8-diyl)bis(propane-3,1-diyl))diguanidine) with the lowest LUMO has the potential ability to receive electrons more than other studied compounds (Figure 3) Semire et al. [19] also reported that, the lower the energy gap, the higher the ability of the studied compounds to react than other studied compounds; therefore, compound 3 proved to have higher potential strength to react than other studied compounds.

Table 2.
Calculated descriptors from the studied compounds.

	E_{HOMO} (eV)	E_{LUMO} (eV)	Energy Gap (eV)
1	–5.48	–0.76	4.72
2	–6.05	–0.83	5.22
3	–5.18	–0.91	4.27
4	–5.18	–0.79	4.39
5	–5.97	–1.00	4.97
6	–5.87	–0.77	5.10
7	–5.87	–0.85	5.02
8	–5.87	–0.74	5.13
9	–5.94	–0.93	5.01
10	–5.89	–1.04	4.85
11	–5.57	–0.43	5.14

Table 3.
Pictorial representation of HOMO-LUMO overlay.

	E_{HOMO} (eV)	E_{LUMO} (eV)
1		
2		

6		
7		
8		

9		
10		
11		
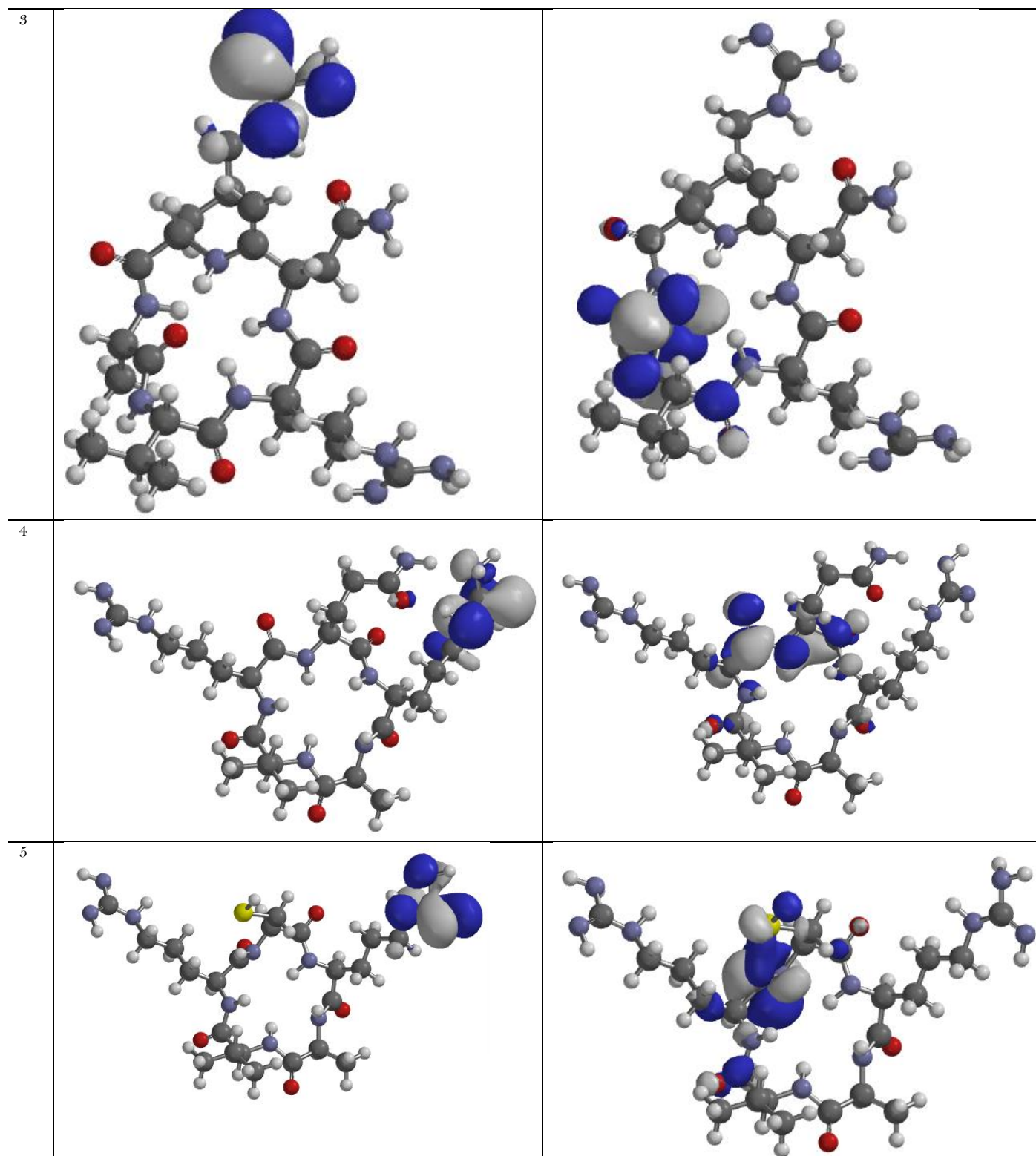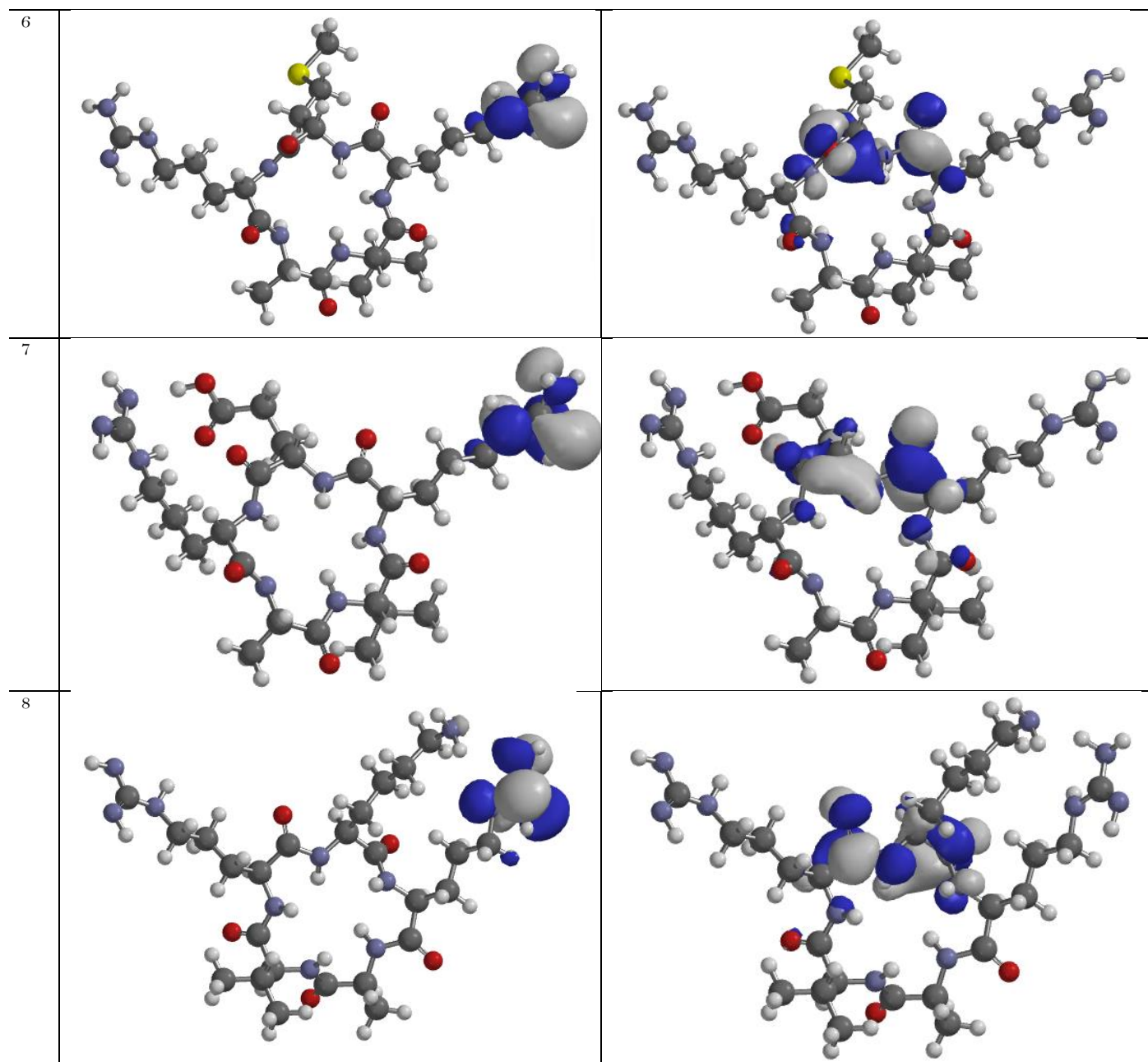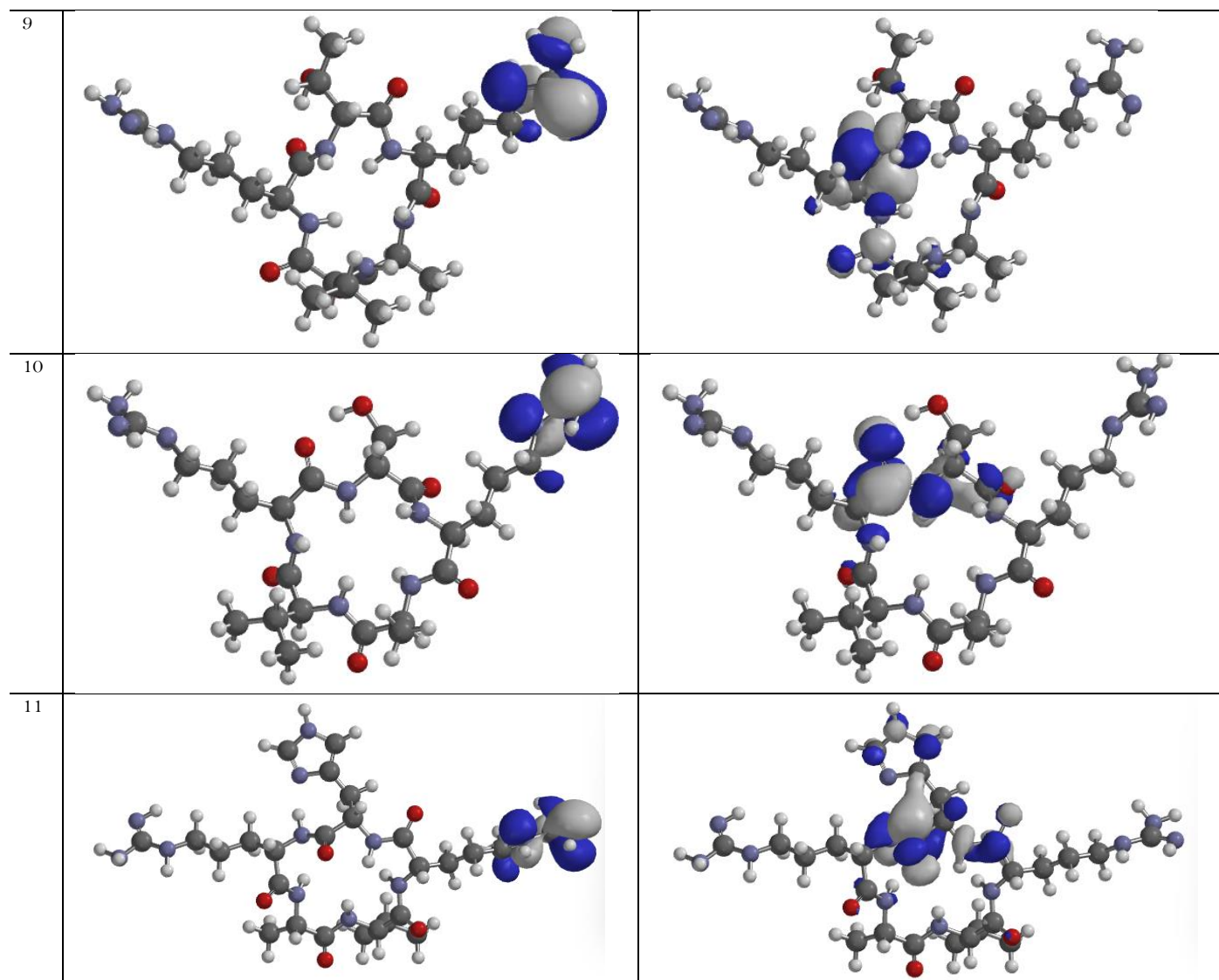
3.2. Molecular Docking Analysis

The inhibiting activity of the eleven compounds was examined via induced fit docking against thymidylate kinase from gram-positive bacteria (4HLC) and gyrase B from Thermus thermophilus (1KIJ). Table 4 presents the inhibiting activity of the eleven compounds via induced fit docking against thymidylate kinase from gram-positive bacteria (4HLC) and gyrase B from Thermus thermophilus (1KIJ), and compares the inhibiting capacity of the lead compound to the cephalosporins (reference compound). It is observed that all the studied compounds exhibit greater strength against the studied receptors, while the reference compound possesses lesser capability.

More so, examination of each of the calculated binding affinities exposed the efficiency of compounds **9** and **5** against thymidylate kinase from gram-positive bacteria (4HLC) and gyrase B from *Thermus thermophilus* (1KIJ), respectively. The amino acids involved in the interaction between the compound 9-4HLC complex were ARG 48, ARG 36, SER 69, and atoms O7, O24, O29 involved in the

interaction, which resulted in lower binding affinity values. Additionally, GLU 41, GLU 49, VAL 110, ASN 45, and atoms C26, N38, S39, O24 from compound 5 were involved in the interaction. Therefore, the efficiency of compounds 9 and 5 could be attributed to the type and position of atoms in each ligand (Figure 1) (Tables 5-7). Furthermore, the comparisons of the inhibitory effects of the studied compounds against the two receptors are displayed in Figure 2.

Table 4.
Calculated Scoring of docked studied compounds.

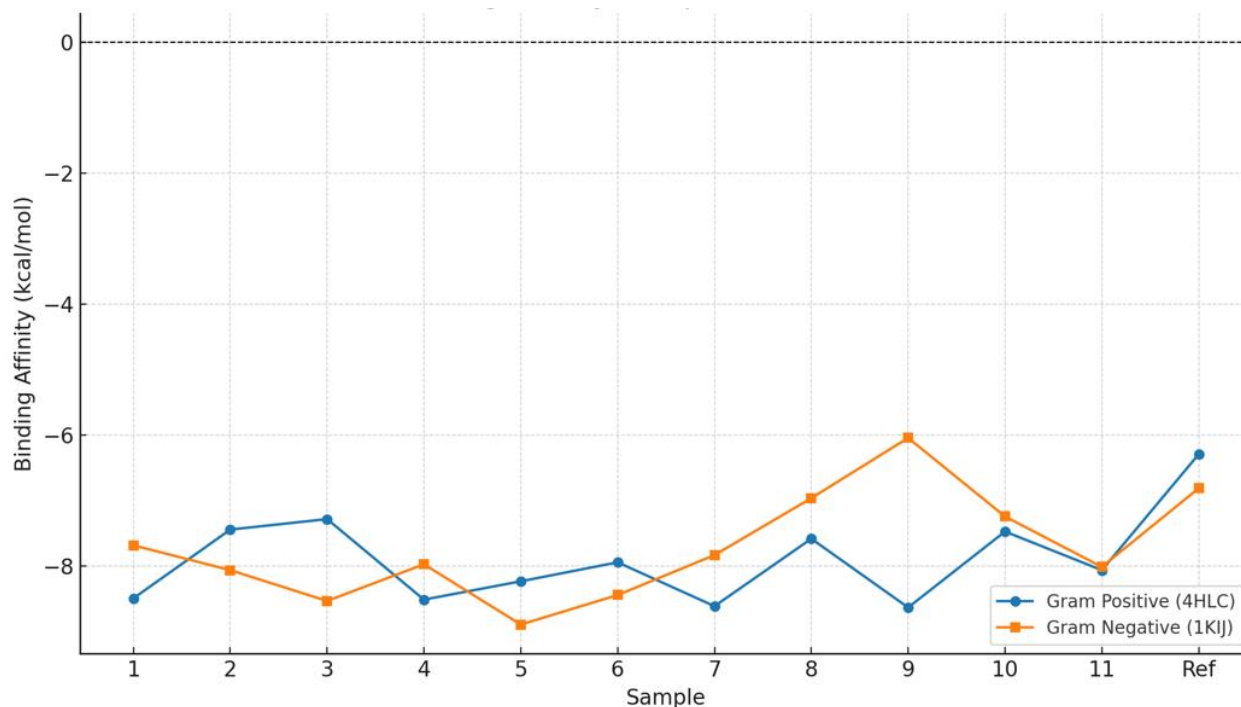|	Gram Positive (4HLC)	Gram Negative (1KIJ)
	Binding Affinity (kcal/mol)	Binding Affinity (kcal/mol)
1	-8.49	-7.68
2	-7.44	-8.06
3	-7.28	-8.53
4	-8.51	-7.97
5	-8.23	-8.89
6	-7.94	-8.44
7	-8.61	-7.83
8	-7.58	-6.96
9	-8.63	-6.04
10	-7.47	-7.24
11	-8.06	-8.01
ref	-6.29	-6.81

Note: Ref: Cephalosporins.

Figure 1.
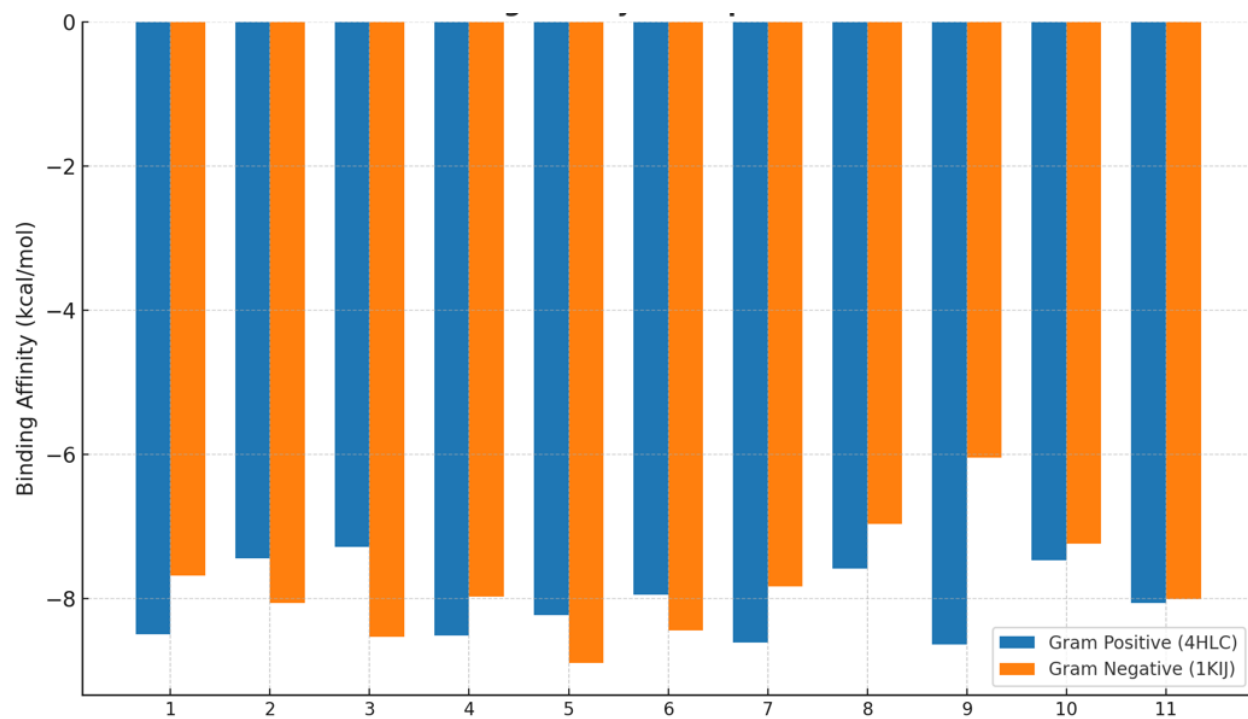Binding Affinity Comparison (kcal/mol).

Figure 2.
Binding Affinity – Grouped Bar Chart.

Table 5.
Types of interactions involved in the studied compounds against 4HLC.

|	Ligand	Receptor	Interaction	Distance	E (kcal/mol)
1	O 7	NE ARG 36 (A)	H-acceptor H-	3.08	-1.5
	O 13	NE ARG 48 (A)	acceptor H-	2.95	-1.7
	O 13	NH2 ARG 48 (A)	acceptor H-	2.67	-2.9
	N 46	NH2 ARG 92 (A)	acceptor	3.37	-0.6
2	N 40	OE1 GLU 62 (A) NE	H-donor H-	2.94	-0.6
	N 39	ARG 105 (A)	acceptor	2.92	-1.4
3	C 9	OE2 GLU 11 (A) OG1	H-donor H-	3.02	-0.8
	N 40	THR 17 (A) NZ LYS	donor H-	2.97	-1.5
	O 12	15 (A) NH2 ARG 92	acceptor H-	3.06	-1.8
	O 12	(A) N GLY 14 (A)	acceptor H-	2.78	-4.0
	O 28		acceptor	3.14	-1.2
4	N 21	OE1 GLN 101 (A)	H-donor H-	2.92	-2.6
	O 30	NH2 ARG 48 (A)	acceptor	2.82	-1.3
5	N 22	OD2 ASP 91 (A)	H-donor	3.11 '	-1.5
	N 38	OE1 GLU 62 (A)	H-donor H-	3.12	-2.9
	O 13	NZ LYS 15 (A)	acceptor H-	3.02	-4.2
	O 29	CB SER 96 (A)	acceptor	3.35	-0.6
6	-	-	-	-	-
7	O 30	NZ LYS 15 (A) NH2	H-acceptor H-	3.25	-3.0
	O 30	ARG 92 (A)	acceptor H-	3.18	-2.7
	N 38	CD ARG 36 (A)	acceptor H-	3.44	-0.6
	N 38	NH2 ARG 36 (A)	acceptor	2.86	-5.2
8	N 21	OE2 GLU 37 (A) OE2	H-donor H-	2.63	-3.0
	C 33	GLU 11 (A)	donor H-	3.15	-0.5
	N 43	NE ARG 105 (A)	acceptor H-	3.55	-1.2
	N 43	NH2 ARG 105 (A)	acceptor H-pi	3.51	-1.4
	N 39	6-ring TYR 100 (A)		3.75	-1.6
9	O 7	NH2 ARG 48 (A)	H-acceptor H-	3.56	-0.5
	O 24	CD ARG 36 (A)	acceptor H-	3.24	-0.9
	O 29	OG SER 69 (A)	acceptor	3.28	-0.5
10	N 22	OE2 GLU 11 (A) NZ	H-donor H-	3.12	-1.1
	O 2	LYS 15 (A)	acceptor	3.49	-1.4
11	O 7	NE ARG 48 (A)	H-acceptor H-	3.11	-0.5
	O 7	NH2 ARG 48 (A) 6-ring	acceptor H-pi	2.83	-3.8
	N 35	PHE 66 (A) 6-ring TYR	H-pi	3.55	-0.6
	N 38	100 (A)		3.46	-0.7

Table 6.
Types of interactions involved in the studied compounds against 1KIJ.

|	Ligand	Receptor	Interaction	Distance		E (kcal/mol)
1	N 19	O GLY 113 (A)	H-donor H-	3.05		-1.4
	N 47	O GLU 104 (A) N	donor H-	3.00		-2.2
	O 13	GLY 116 (A)	acceptor	3.14		-1.3
2	N 13	O LEU 114 (A) O	H-donor H-	3.27		-0.7
	N 13	GLY 116 (A) O LYS	donor H-	3.23		-0.9
	N 21	109 (A) O VAL 110	donor H-	3.07		-0.6
	N 21	(A) O GLU 104 (A)	donor H-	3.20		-0.6
	N 40	N GLY 116 (A) NZ	donor	3.12		-0.5
	O 2	LYS 109 (A) 5-ring HIS	H-acceptor	2.95		-2.0
	O 28	98 (A)	H-acceptor	2.74		-6.3
	C 4		H-pi	4.66		-1.2
3	O 12	OG SER 111 (A)	H-acceptor H-	3.13		-1.5
	O 28	N GLY 112 (A)	acceptor	3.13		-1.6
4	N 21	OD2 ASP 48 (A)	H-donor H-	3.19		-2.2
	O 23	NE2 GLN 105 (A) N	acceptor H-	2.97		-1.2
	O 42	LYS 109 (A)	acceptor	3.27		-0.7
5	C 26	OE2 GLU 41 (A)	H-donor H-	3.46		-0.9
	N 38	OE2 GLU 49 (A)	donor	3.26		-0.7
	S 39	O VAL 110 (A)	H-donor	3.12		-1.4
	O 24	ND2 ASN 45 (A)	H-acceptor	2.84		-0.8
6	C 14	O VAL 110 (A) OE1	H-donor H-	3.38		-0.7
	C 17	GLU 41 (A)	donor H-	3.30		-0.6
	N 18	O SER 111 (A)	donor H-	2.90		-0.9
	O 23	N GLY 112 (A)	acceptor	3.05		-0.6
	O 23	NZ LYS 337 (A)	H-acceptor H-	3.11		-0.7
	O 28	OG SER 111 (A)	acceptor	3.18		-0.6
	S 39	CA HIS 115 (A) N	H-acceptor	3.77		-0.8
	S 39	GLY 116 (A)	H-acceptor	3.20		-3.4
7	N 21	O GLY 113 (A)	H-donor H-	3.32		-1.4
	N 39	O GLU 104 (A)	donor H-	3.09	3.03	-1.4
	N 39	O ALA 107 (A) N	donor	3.18		-1.4
	O 7	GLY 116 (A)	H-acceptor H-	3.13		-1.0
	O 12	N GLY 113 (A)	acceptor			-0.6
8	N 8	OE1 GLU 265 (A)	H-donor	2.96		-1.7
	N 13	OE1 GLU 265 (A)	H-donor	3.15		-3.9
	N 21	OE1 GLU 193 (A)	H-donor	3.10	2.86	-2.8
	O 12	NH2 ARG 276 (A)	H-acceptor			-1.2
9	C 26	OE1 GLU 265 (A)	H-donor H-	3.09		-2.2
	N 30	OE2 GLU 265 (A)	donor	3.50		-1.3
10	N 30	O ILE 266 (A) O	H-donor H-	3.01		-4.8
	O 39	ILE 266 (A)	donor	2.75		-0.8
11	N 22	OE1 GLU 193 (A) O	H-donor H-	3.22		-0.8
	N 35	GLY 113 (A) O MET	donor	3.13	3.33	-0.9
	N 38	25 (A) NH1 ARG 276	H-donor H-	3.34		-1.1
	N 21	(A) N HIS 115 (A)	acceptor H-	3.28		-1.2
	N 37		acceptor			-2.0

Table 7.
Pictorial representation of the interaction between studied ligands and the receptors.
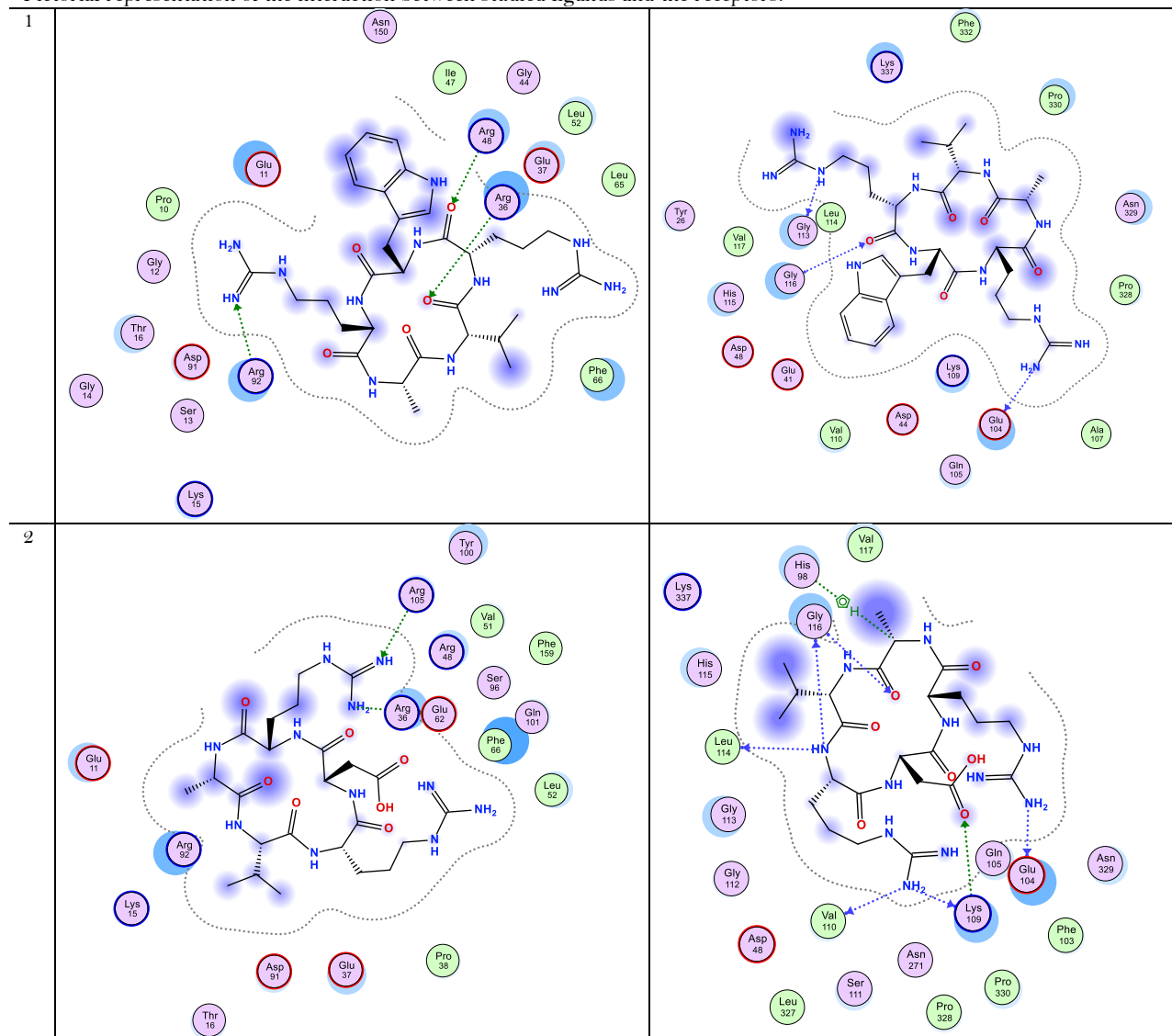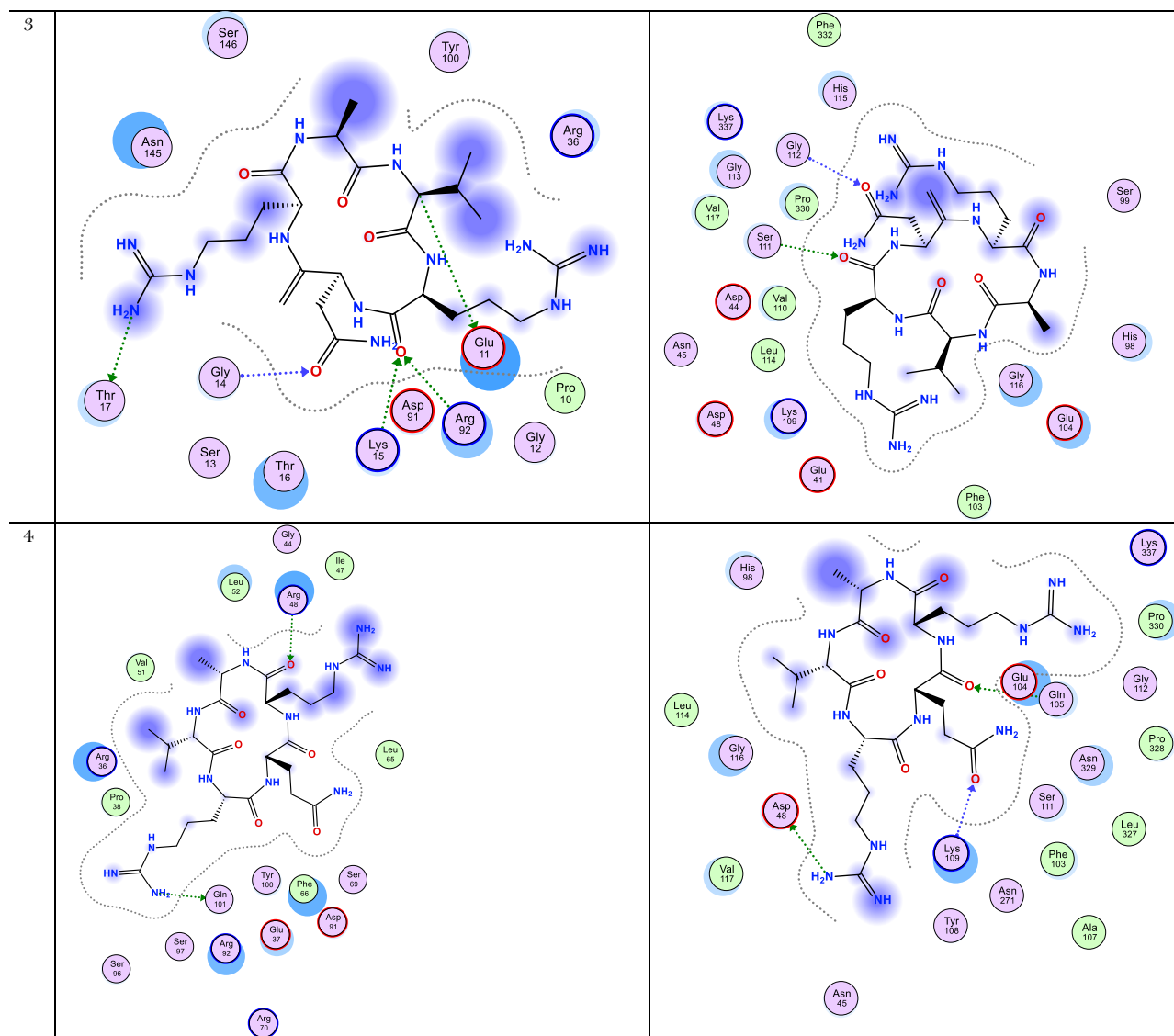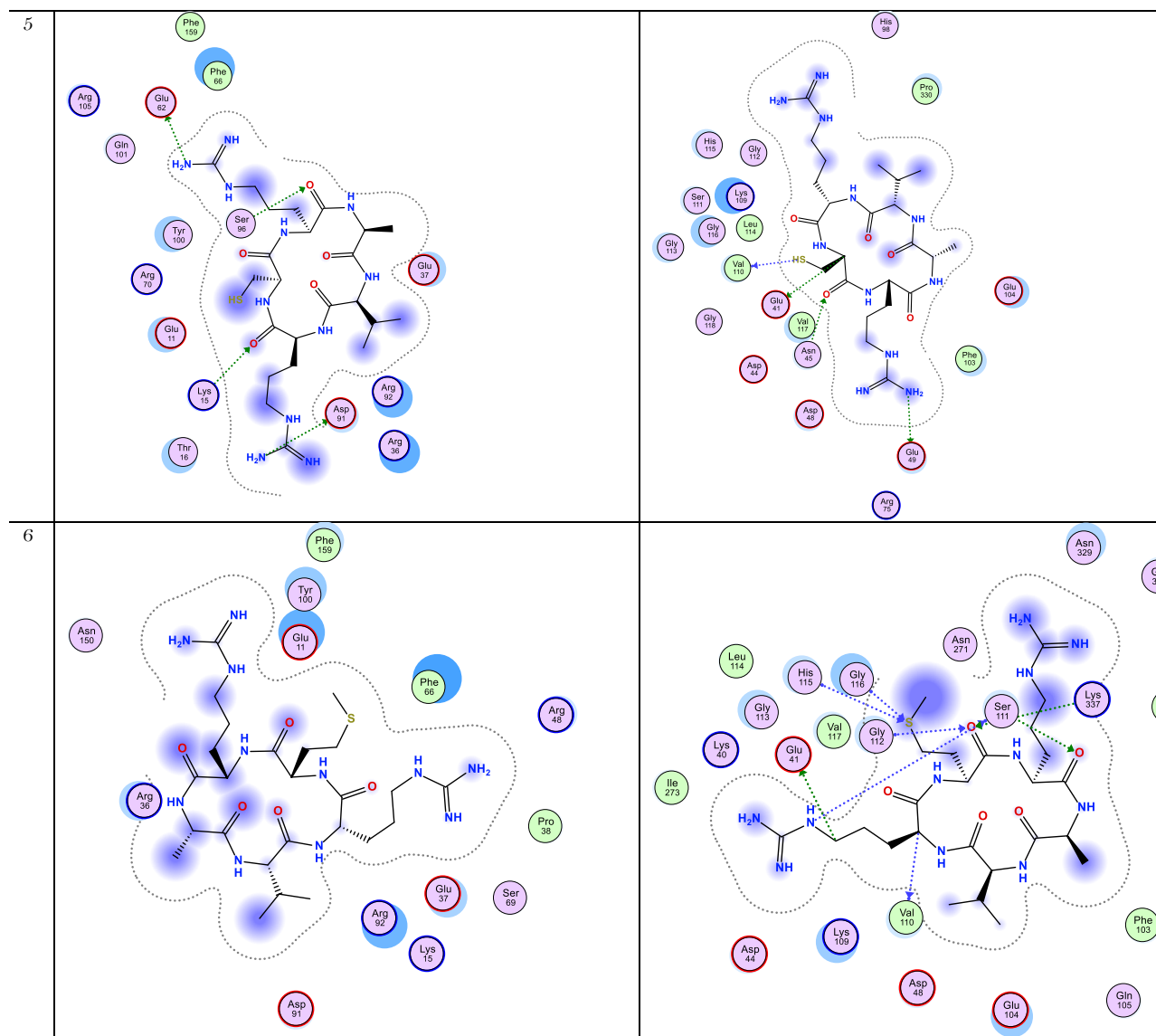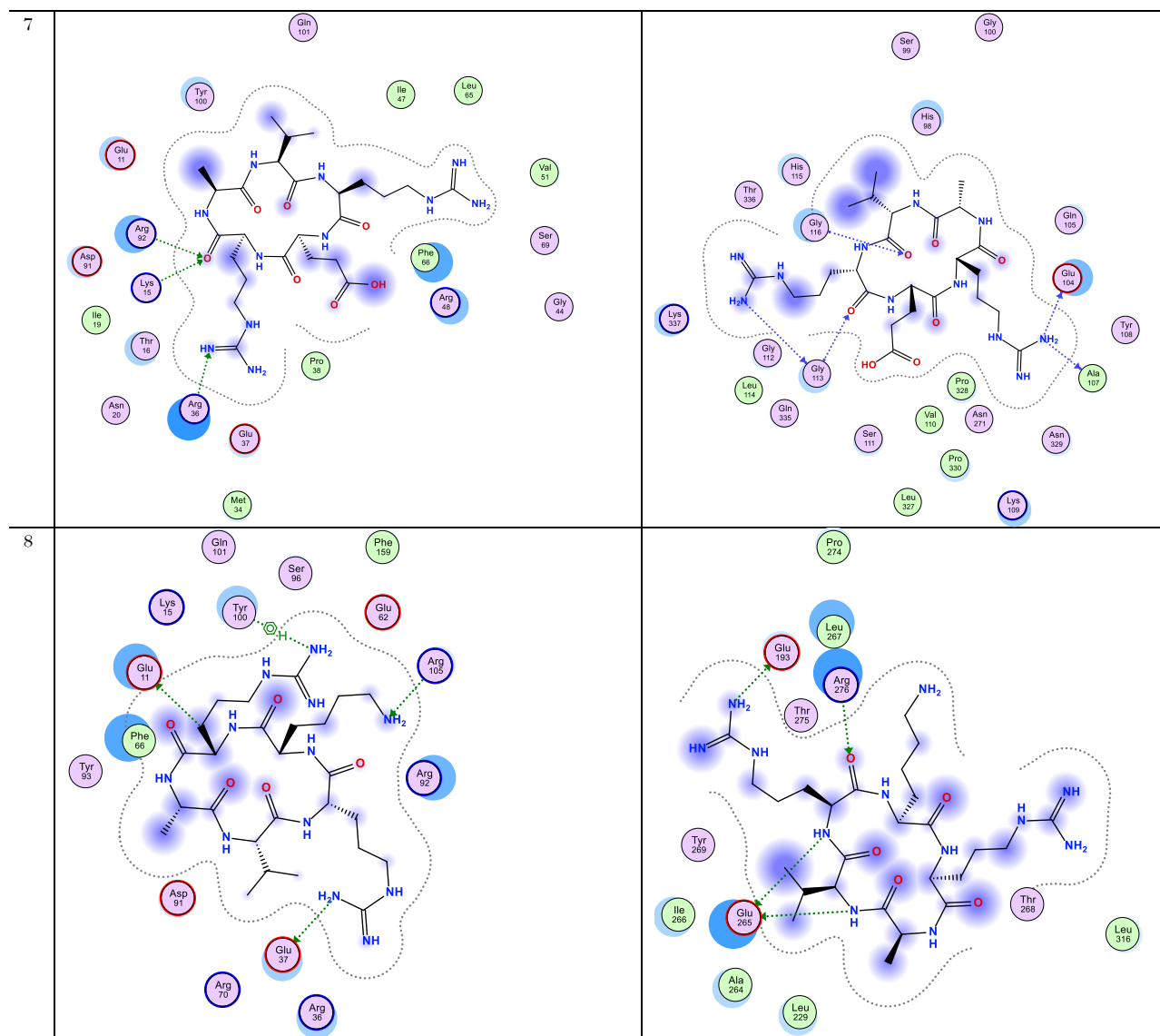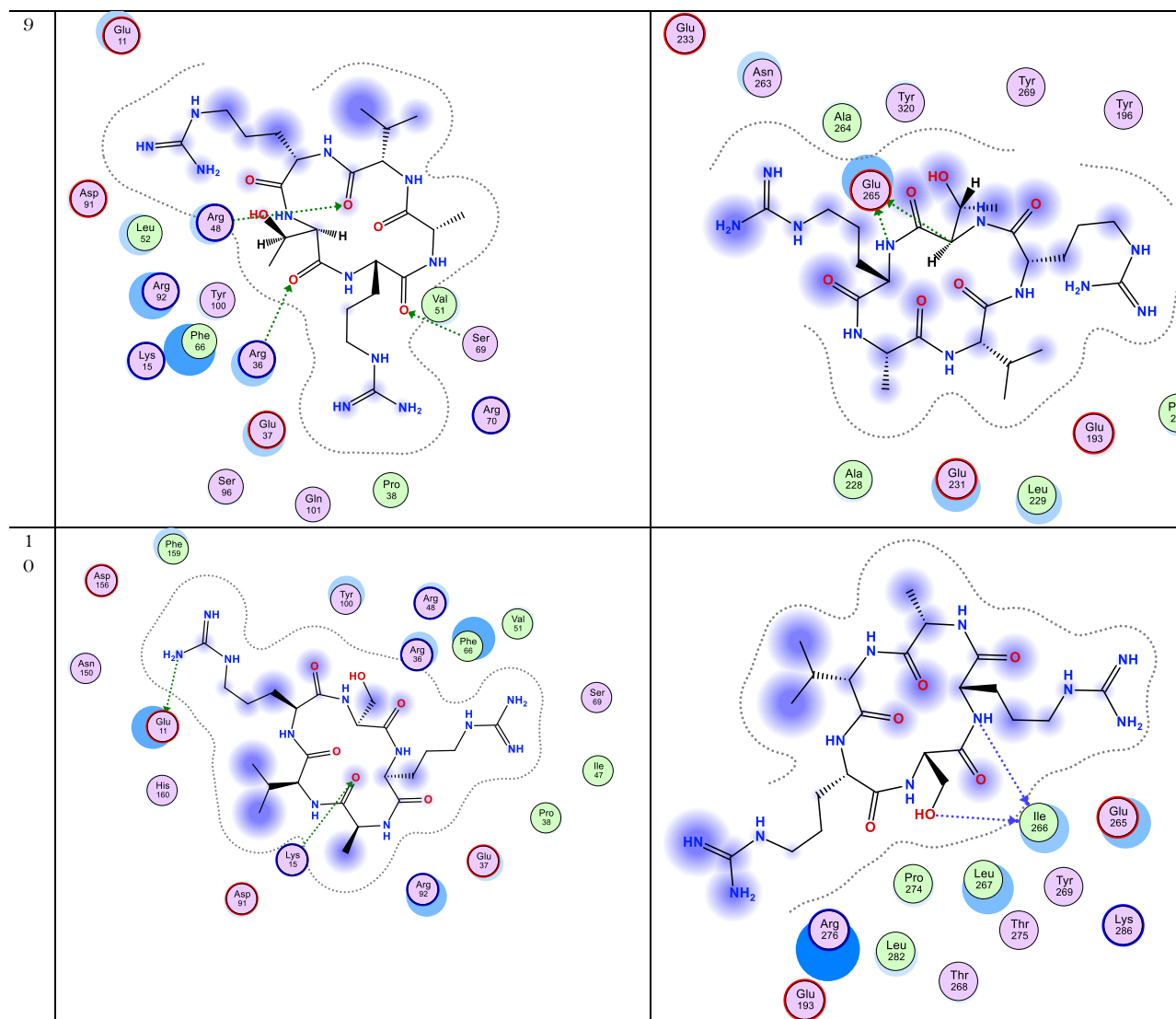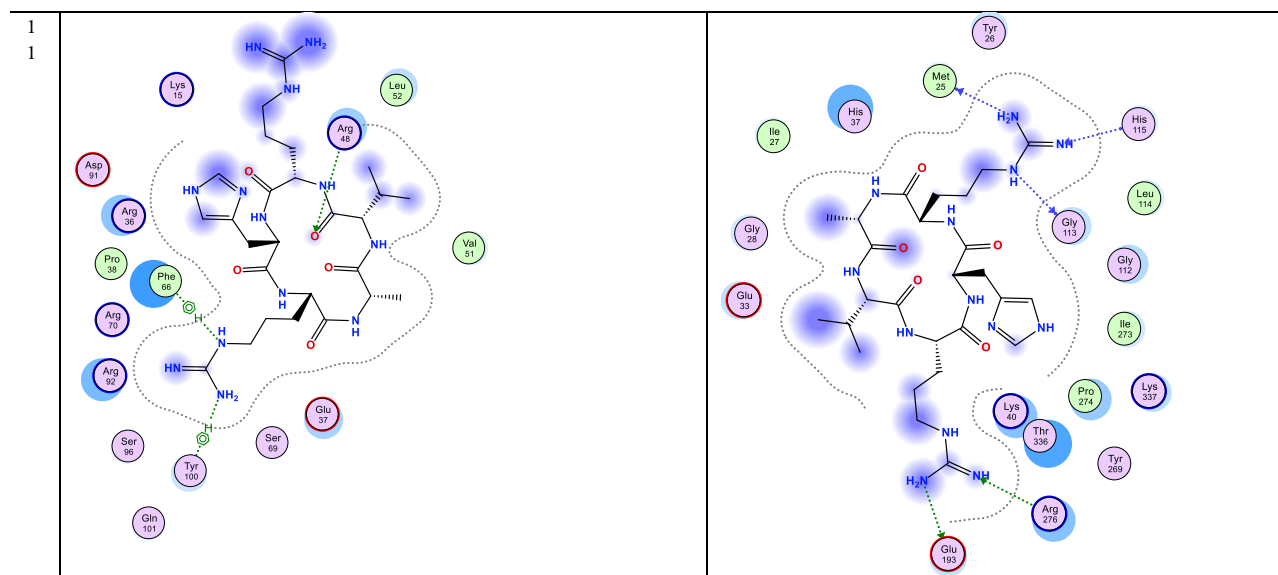
3.3. Binding Affinity Prediction Evaluation

The Decision Tree Regressor trained using EHOMO, ELUMO, and ΔE effectively developed a predictive model for binding affinity against the examined bacterial targets. The enhanced model, discovered through Grid Search with Leave-One-Out Cross-Validation (LOOCV), produced a Mean Absolute Error (MAE) of 0.53 kcal/mol and a Coefficient of Determination (R^2) of −0.86. Despite the negative R^2 value, which reflects the limited dataset size (n = 11) and the model's restricted generalizability, the Decision Tree offered significant insights into structure–activity relationships (SAR) (Figure 3).

3.4. Significant Descriptor Examination

An examination of feature importance derived from the model indicated that the energy gap (ΔE) was the primary descriptor, accounting for roughly 60% of the predictive effectiveness. This observation is consistent with established quantum chemical principles, which suggest that a smaller energy gap is typically associated with heightened reactivity and enhanced binding interactions. ELUMO represented around 34% of the influence, highlighting the importance of electron-accepting ability in the affinity between ligands and targets, especially in peptide-enzyme interactions. EHOMO had the least impact (approximately 6%), indicating that the capability to donate electrons was less directly tied to the docking scores observed in this particular dataset. Significantly, compounds demonstrating strong binding affinity, Compound 9 (−8.63 kcal/mol) for Gram-positive 4HLC and Compound 5 (−8.89 kcal/mol) for Gram-negative 1KIJ, showed advantageous ΔE values alongside well-balanced HOMO/LUMO energies. This alignment between docking outcomes and feature importance derived from machine learning enhances the credibility of the SAR analysis (Figures 4, 5; Table 8).
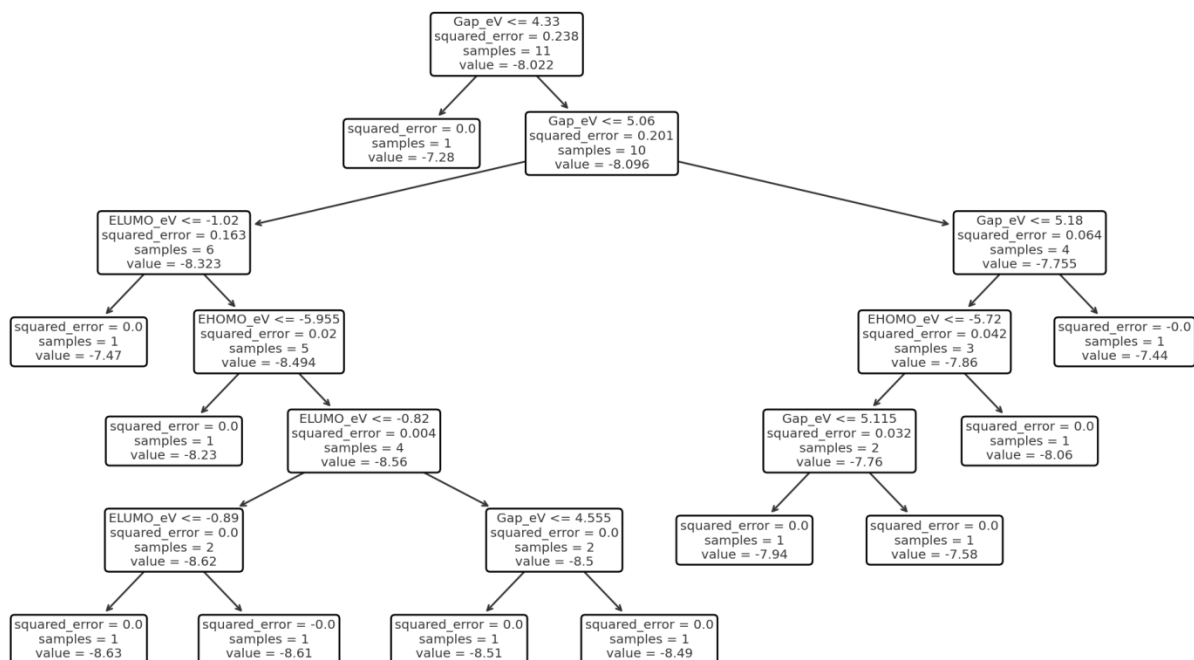
Best Decision Tree Structure

Figure 3.
Decision tree structure.

Table 8.
LOOCV Predictions and Errors

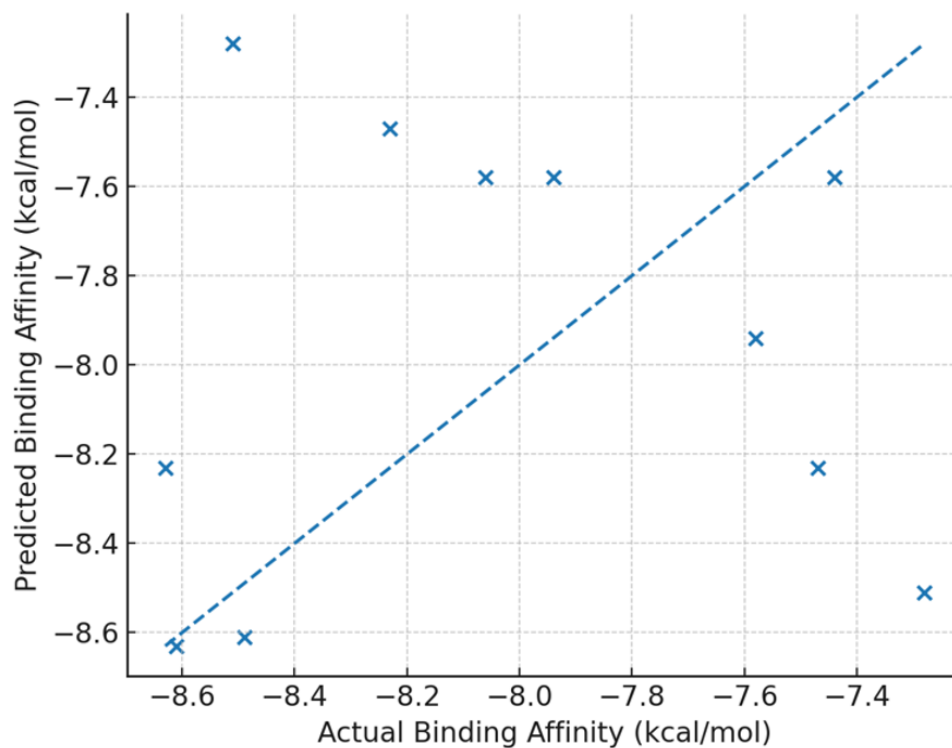| Sample	EHOMO (eV)	ELUMO (eV)	Energy Gap (eV)	Binding (kcal/mol)	Predicted Binding CV	Absolute Error
1	-5.48	-0.76	4.72	-8.49	-8.61	0.12
2	-6.05	-0.83	5.22	-7.44	-7.58	0.14
3	-5.18	-0.91	4.27	-7.28	-8.51	1.23
4	-5.18	-0.79	4.39	-8.51	-7.28	1.23
5	-5.97	-1	4.97	-8.23	-7.47	0.76
6	-5.87	-0.77	5.1	-7.94	-7.58	0.36
7	-5.87	-0.85	5.02	-8.61	-8.63	0.02
8	-5.87	-0.74	5.13	-7.58	-7.94	0.36
9	-5.94	-0.93	5.01	-8.63	-8.23	0.4
10	-5.89	-1.04	4.85	-7.47	-8.23	0.76
11	-5.57	-0.43	5.14	-8.06	-7.58	0.48

Figure 4.
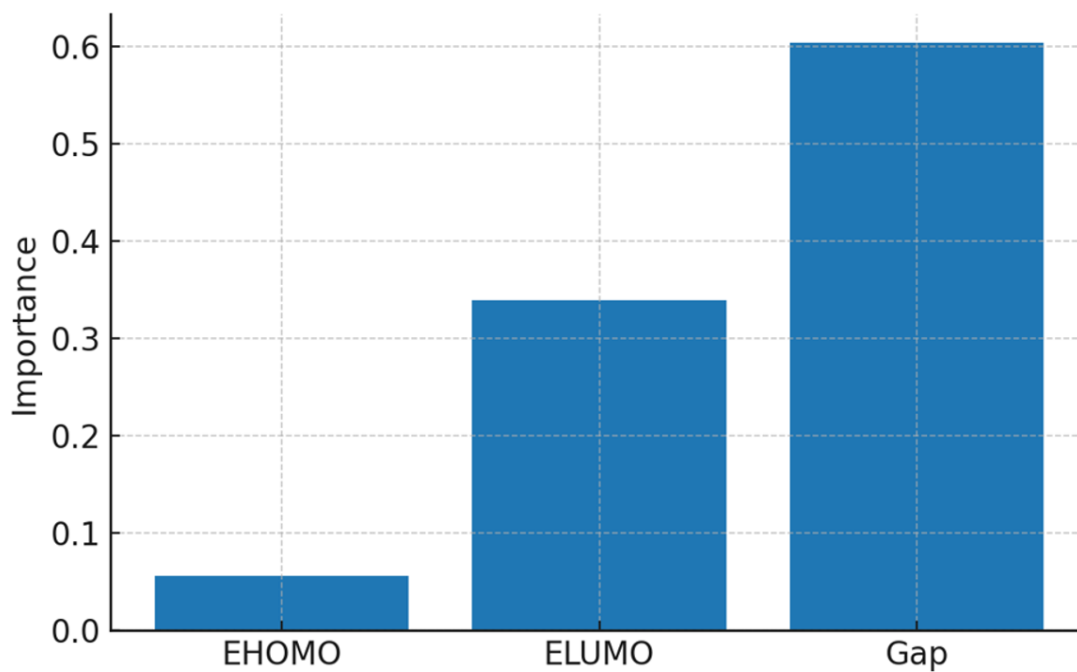Actual vs Predicted (Decision Tree, LOOCV).

Figure 5.
Decision Tree Feature Importance.

4. Conclusions

In this study, ARG-TRP-ARG-based peptides were analyzed using a computational method. The attributes derived from the optimized compounds indicated the reactivity levels of those compounds. Compounds 3 and 4 displayed a strong tendency to react in terms of HOMO energy, while compound 3 showed a notable propensity for reaction concerning its energy gap. It was determined that compound 10, which had the lowest LUMO energy value, demonstrated the greatest capacity to accept electrons from adjacent compounds. Furthermore, when all the compounds were docked against thymidylate kinase from gram-positive bacteria (4HLC) and gyrase B from Thermus thermophilus (1KIJ), compounds 9 and 5 showed greater inhibitory effects on the studied receptors compared to the other compounds, respectively. The effectiveness of the lead compounds was further verified through molecular dynamics simulations, which confirmed that these lead compounds had a superior ability to inhibit the studied receptors relative to the reference compound.

Funding:

Transparency:

The authors confirm that the manuscript is an honest, accurate, and transparent account of the study; that no vital features of the study have been omitted; and that any discrepancies from the study as planned have been explained. This study followed all ethical practices during writing.

Copyright:

References

[1]   A. C.-L. Lee, J. L. Harris, K. K. Khanna, and J.-H. Hong, "A comprehensive review on current advances in peptide drug development and design," *International Journal of Molecular Sciences*, vol. 20, no. 10, p. 2383, 2019. https://doi.org/10.3390/ijms20102383

[2]   Y. Gao, X. Yuan, Z. Zhu, D. Wang, Q. Liu, and W. Gu, "Research and prospect of peptides for use in obesity treatment," *Experimental and Therapeutic Medicine*, vol. 20, no. 6, p. 234, 2020. https://doi.org/10.3892/etm.2020.9364

[3]   N. Bilousova, N. Tkachenko, N. Kozhuharyova, and M. Dolzhenko, "Research of affordability to essential medicines for coronary heart disease in Ukraine," *Journal of Pharmaceutical Policy and Practice*, vol. 18, no. 1, p. 2470841, 2025. https://doi.org/10.1080/20523211.2025.2470841

[4]   J. J. Majura *et al.*, "The current research status and strategies employed to modify food-derived bioactive peptides," *Frontiers in Nutrition*, vol. 9, p. 950823, 2022. https://doi.org/10.3389/fnut.2022.950823

[5]   O. W. Press *et al.*, "Phase II trial of 131I-B1 (anti-CD20) antibody therapy with autologous stem cell transplantation for relapsed B cell lymphomas," *The Lancet*, vol. 346, pp. 336–340, 1995.

[6]   C. A. Brizuela, G. Liu, J. M. Stokes, and C. de la Fuente-Nunez, "AI methods for antimicrobial peptides: progress and challenges," *Microbial Biotechnology*, vol. 18, no. 1, p. e70072, 2025. https://doi.org/10.1111/1751-7915.70072

[7]   I. E. Mba and E. I. Nweze, "Antimicrobial peptides therapy: An emerging alternative for treating drug-resistant bacteria," *The Yale Journal of Biology and Medicine*, vol. 95, no. 4, pp. 445–463, 2022.

[8]   Centers for Disease Control and Prevention (CDC), "Antibiotic resistance threats in the United States," 2022. https://www.cdc.gov/

[9]   L. Bonadonna, R. Briancesco, and A. M. Coccia, *Analysis of microorganisms in hospital environments and potential risks. Indoor Air Quality in Healthcare Facilities*. Cham: Springer, 2017.

[10]   K. Lindström and S. A. Mousavi, "Effectiveness of nitrogen fixation in rhizobia," *Microbial Biotechnology*, vol. 13, no. 5, pp. 1314-1335, 2020. https://doi.org/10.1111/1751-7915.13517

[11] B. Iqbal *et al.*, "Advancing environmental sustainability through microbial reprogramming in growth improvement, stress alleviation, and phytoremediation," *Plant Stress*, vol. 10, p. 100283, 2023. https://doi.org/10.1016/j.stress.2023.100283

[12] S. Zhang *et al.*, "Molecular methods for pathogenic bacteria detection and recent advances in wastewater analysis," *Water*, vol. 13, no. 24, p. 3551, 2021. https://doi.org/10.3390/w13243551

[13] G. Martínez-Botella *et al.*, "Sulfonylpiperidines as novel, antibacterial inhibitors of Gram-positive thymidylate kinase (TMK)," *Bioorganic & Medicinal Chemistry Letters*, vol. 23, no. 1, pp. 169-173, 2013.

[14] V. Lamour, L. Hoermann, J.-M. Jeltsch, P. Oudet, and D. Moras, "An open conformation of the thermus thermophilusGyrase B ATP-binding domain," *Journal of Biological Chemistry*, vol. 277, no. 21, pp. 18947-18953, 2002.

[15] L. Qin, Y. X. Zhao, Y. N. Wang, J. L. An, Q. Liu, and H. G. Zheng, "The effects of ligands with different electron donation on the nitrogen reduction performance of constructed Co-MOFs: NH_3 or N_2H_4?," *Small Methods*, vol. 9, no. 5, p. 2401603, 2025. https://doi.org/10.1002/smtd.202401603

[16] Z. Yin, W. Song, B. Li, F. Wang, L. Xie, and X. Xu, "Neural networks prediction of the protein-ligand binding affinity with circular fingerprints," *Technology and Health Care*, vol. 31, no. 1_suppl, pp. 487-495, 2023. https://doi.org/10.3233/THC-236042

[17] F. Leidner, N. Kurt Yilmaz, and C. A. Schiffer, "Target-specific prediction of ligand affinity with structure-based interaction fingerprints," *Journal of Chemical Information and Modeling*, vol. 59, no. 9, pp. 3679-3691, 2019. https://doi.org/10.1021/acs.jcim.9b00457

[18] A. Choudhary, R. W. Newberry, and R. T. Raines, "n→ π* interactions engender chirality in carbonyl groups," *Organic Letters*, vol. 16, no. 13, pp. 3421-3423, 2014. https://doi.org/10.1021/ol5012967

[19] B. Semire, A. Oyebamiji, and M. Ahmad, "Theoretical study on structure and electronic properties of 2, 5-bis [4-N, N-diethylaminostyryl] thiophene and its furan and pyrrole derivatives using density functional theory (DFT)," *Pakistan Journal of Chemistry*, vol. 2, no. 4, pp. 166-173, 2012.